ELSEVIER

Journal of Nuclear Materials 258–263 (1998) 205–214

journal of nuclear materials

Research and development on vanadium alloys for fusion applications

S.J. Zinkle [a,*], H. Matsui [b], D.L. Smith [c], A.F. Rowcliffe [a], E. van Osch [d], K. Abe [e], V.A. Kazakov [f]

[a] Metals and Ceramics Division, Oak Ridge National Laboratory, P.O. Box 2008, Oak Ridge, TN 37831-6376, USA
[b] Institute for Materials Research, Tohoku University, Sendai 980-77, Japan
[c] Argonne National Laboratory, Argonne, IL 60439, USA
[d] Netherlands Energy Research Foundation ECN, 1755 ZG Petten, The Netherlands
[e] Department of Quantum Science and Energy Engineering, Tohoku University, Sendai 980-77, Japan
[f] Research Institute of Atomic Reactors, Dimitrovgrad, Russian Federation

Abstract

The current status of research and development on unirradiated and irradiated V–Cr–Ti alloys intended for fusion reactor structural applications is reviewed, with particular emphasis on the flow and fracture behavior of neutron-irradiated vanadium alloys. Recent progress on fabrication, joining, oxidation behavior, and the development of insulator coatings is also summarized. Pronounced flow localization and loss of strain hardening capacity with uniform elongations <1% generally occurs in vanadium alloys for irradiation temperatures below ~400°C (0.31 T_M). These changes in tensile properties for T_{irr} < 400°C are generally accompanied by large increases in the ductile-to-brittle transition temperature measured under both dynamic and quasi-static loading conditions. The relationships between radiation hardening, flow localization, strain rate, and fracture properties are examined. The irradiated mechanical properties at temperatures between 430°C and 650°C are acceptable for most structural applications. Further work is needed to determine how far the allowable lower and upper operating temperature limits can be expanded beyond the 430–650°C range.

1. Introduction

Alloys based upon the V–Cr–Ti system are attractive candidates for structural applications in fusion systems because of their low activation properties, high thermal stress factor, good strength at elevated temperatures, and good compatibility with liquid lithium. Many of the advantages and disadvantages associated with vanadium alloys have been summarized in previous review papers [1–6]. Recent work has shown that unirradiated V–(3–6%) Cr–(3–6%) Ti alloys have favorable mechanical properties and can be fabricated into tubes and other engineering-relevant shapes. In addition, considerable advances have been made in the past few years on joining techniques for vanadium alloys. On the other hand, considerable work is still needed in order to develop a viable self-healing insulator coating for the liquid metal coolant.

The purpose of this review is to summarize the current status of research and development on unirradiated and irradiated vanadium alloys intended for fusion reactor structural applications. Particular emphasis will be placed on the flow and fracture behavior of unirradiated and neutron-irradiated vanadium alloys, where a significant advancement in the knowledge of the physical metallurgy processes has been accumulated in the past few years.

2. Fabrication and physical metallurgy of unirradiated alloys

One of the often-cited disadvantages associated with vanadium alloys is the lack of a large industrial

* Corresponding author. Tel.: +1 423 576 7220; fax: +1 423 574 0641; e-mail: zinklesj@ornl.gov.

0022-3115/98/$19.00
PII: S 0 0 2 2 - 3 1 1 5 (9 8) 0 0 2 6 9 - 4

infrastructure. Up until recent times, essentially all data on vanadium alloys had been generated on small laboratory heats with typical masses of 1–50 kg. Since vanadium alloys are sensitive to interstitial impurity concentrations, an open question remained whether satisfactory properties could be obtained on large alloy heats. Two different V–4Cr–4Ti alloy heats with masses of 500 [4] and 1200 kg [7] have recently been fabricated. The fabrication of the larger vanadium alloy heat was stimulated by a program which will install a V–4Cr–4Ti radiative divertor structure into the DIII-D Tokamak at General Atomics in late 1998 [7]. Impurity pickup in these large heats was determined to be comparable to that in previous small laboratory heats of vanadium alloys, and the unirradiated mechanical properties were also in agreement with data obtained on small heats. The fabrication of a wide variety of product forms, including thin walled tubing, has been demonstrated.

Several recent studies on the tensile properties of vanadium alloys containing 4–5% Cr and Ti have been performed [4,8–12]. A typical feature in the load-elongation curves is the appearance of serrations in the work-hardening portion of the curve at test temperatures above ~300°C. This so-called dynamic strain aging effect is associated with the migration of the interstitial solute atoms to dislocations during the deformation, and is a common feature in body-centered cubic metals including pure vanadium [13]. Several different types of serrated yielding occur, depending on the test temperature. Serrations which fluctuate about the mean of the load-elongation curve ("type A" behavior, occurring at 300–400°C in V–4Cr–4Ti tested at a strain rate of 1×10^{-3} s^{-1}) are associated with O, C solute, whereas serrations which occur below the mean of the load-elongation curve ("type C" behavior, present at tensile test temperatures above 500°C) also involve diffusion of N [9,10]. The appearance of dynamic strain aging is accompanied by a shift in the hardening strain rate exponent from the positive values which occur at tensile test temperatures below ~300°C (for strain rates above 1×10^{-3} s^{-1}) to negative values at high test temperatures and slow strain rates [10].

The typical matrix concentration of dissolved interstitial solutes in the present generation of V–(4–5%) Cr–(4–5%) Ti alloys can be estimated to be ~400–500 ppm, based on the observation by Satou and Chung [14] that oxycarbonitride precipitates do not form for interstitial solute concentrations below this level (the typical O + C + N solute concentrations in these vanadium alloys range from 400 to 700 ppm). It is worth noting that the addition of interstitial solute gettering species such as Si, Al or Y in concentrations comparable or slightly higher than the interstitial solute concentration can produce a considerable decrease in the dynamic strain aging [11]. This indicates that the matrix concentration of free interstitial solutes has been significantly reduced due to precipitation with the gettering elements. Detailed irradiation tests are needed to determine whether a reduction in the matrix concentration of interstitial solute (with a corresponding increase in the oxycarbonitride precipitate density) is beneficial.

A clear picture of the effect of heat treatment and Cr, Ti solute additions on the impact properties of vanadium alloys has emerged as the result of a series of recent studies [15–19]. The ductile to brittle transition temperature (DBTT) as measured on Charpy vee-notch (CVN) impact specimens increases with both solute content and final heat treatment temperature. As has been emphasized elsewhere [20–24], the measured DBTT also depends strongly on the mechanical constraint present at the tip of the notch. For example, the measured DBTT of V–4Cr–4Ti annealed at 1000°C for 2 h is about −200°C and −150°C, respectively, for machined-notch (root radius of 0.08 mm, 30° notch angle) and precracked CVN specimens [25]. Similar differences in the DBTT of precracked vs. machined-notched CVN specimens have been obtained for other vanadium alloys [15], and even larger differences can be obtained for certain combinations of notch acuity and/or mechanical constraint [20,22,23]. A DBTT of −200°C for V–4Cr–4Ti (heat #832665) was obtained for both machined-notch and precracked CVN specimens in the L–S orientation [18,26], indicating a higher resistance to crack propagation in the short transverse direction compared to the long transverse direction examined in other studies [25,27].

Fig. 1 summarizes the results of a recent study performed on machined-notch CVN specimens with a root radius of 0.08 mm and a 30° notch angle [19]. The data for V–(4–5%) Cr–(4–5%) Ti show that the DBTT increases as the annealing temperature is increased above 1000°C, in agreement with previous studies [5,15,16,18,28]. The DBTT for a given annealing temperature shows an approximately linear increase with

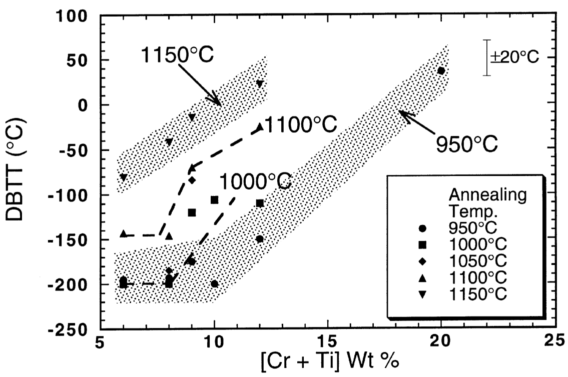

Fig. 1. Effect of annealing temperature and solute additions on the DBTT of V–Cr–Ti alloys [19].

increasing concentration of Cr and Ti solute. This behavior can be explained by well-established stress-controlled cleavage (equivalent yield stress) models [22,24], since the tensile strength of vanadium alloys increases with increasing Cr + Ti content [18]. It should be noted that some early published results on the effect of solute additions on the impact properties of vanadium alloys implied a pronounced "step function" increase in the DBTT for Cr + Ti contents above ~10% [2,3,29]. These results have been cited by some authors as evidence that a dramatic transition in fracture behavior might occur due to transmutation-induced increases in the Cr content of irradiated vanadium alloys [30]. However, the early DBTT studies [2,3,29] used a relatively high annealing temperature of 1125°C for Cr + Ti contents above 10%, and the large reported "step function" increase in DBTT at Cr + Ti contents above 10% can be shown to be largely influenced by annealing temperature effects in addition to solute hardening effects [15]. From Fig. 1 and Ref. [18], it can be seen that the DBTT for vanadium alloys annealed at a given temperature increases steadily with increasing solute content, without any "step function" increases. The physical mechanism responsible for heat treatment sensitivity of the DBTT in vanadium alloys is uncertain, although it is interesting to note that fine-scale precipitation (as monitored by thermal helium desorption spectrometry) apparently disappeared for annealing temperatures of 950–1050°C and reappeared at annealing temperatures $\geqslant$ 1100°C [31].

3. Welding and compatibility

Several different techniques for joining vanadium alloys are being investigated, including gas tungsten arc (GTA) [32,33], electron beam [33,34], laser [34], and inertia [35] welds. One goal of these welding studies is to eliminate the need for post-weld heat treatment procedures, due to the potential problems associated with impurity pickup during elevated temperature annealing in poor vacuum systems. As recently as one year ago, the typical DBTT in as-welded GTA, electron beam and laser weld specimens was 30–250°C, with the highest DBTT associated with GTA welds [32,34]. A considerable reduction in the DBTT of these welds could be achieved by post-weld heat treatment at 950–1000°C in vacuum. Recent work on GTA welds using a Ti getter glovebox system to minimize interstitial solute pickup from the surrounding atmosphere has yielded a DBTT as low as ~50°C in as-welded 6-mm plate material [33]. Similarly, recent electron beam welds have achieved a DBTT as low as −90°C in as-welded material by utilizing a small beam diameter in order to minimize the grain size in the weldment [33]. In both of these cases, the DBTT was not changed by subsequent annealing. This suggests that post-weld heat treatments may not be necessary if the surrounding atmosphere is carefully controlled during the welding process.

Systematic studies have been conducted to investigate the effects of oxygen and oxidation on the microstructure and tensile properties of V–(4–5) Cr–(4–5) Ti alloys [36–40]. It was observed that the grain size of recrystallized material was unaffected by subsequent thermal aging at temperatures up to 850°C for times to 5000 h [37,38]. Adherent oxides were formed upon exposure to air at 500°C. The oxidation kinetics were insensitive to oxygen partial pressure over the investigated range of 10^{-4}–10^{5} Pa, and exhibited logarithmic behavior at 400°C and parabolic kinetics at 500°C [36–38]. Oxygen diffusion as indicated by hardness profile measurements was on the order of 100 μm after 1000 h exposure at 500°C [37]. The post exposure tensile strengths of 1 mm-thick specimens at 20°C and 500°C were not significantly affected by exposure to a range of oxygen pressure (10^{-4}–10^{5} Pa) for 250–275 h. However, significant reductions in total and uniform elongations were observed [36,38,40], particularly in room temperature tensile tests for 500°C exposures over 1000 h [38]. Pre-exposure to oxygen at 500°C was also observed to increase the sensitivity of V–4Cr–4Ti to hydrogen embrittlement [39].

The development of electrically insulating walls for coolant channels is a key feasibility issue for self-cooled liquid metal systems [41]. A self-healing coating is considered to be the most appropriate approach for providing the required insulating characteristics with acceptable reliability on complex channel geometries. Of the several oxides and nitrides that were initially considered for the coating application for the lithium/vanadium system, CaO and AlN have been identified as the leading candidates. Results obtained thus far indicate that AlN coatings formed by physical vapor deposition appear to be compatible with lithium and they exhibit adequate resistivity at room temperature after Li exposure [42]. However, attempts to generate high resistance, stable coatings by exposure to lithium have thus far been unsuccessful. CaO coatings have been formed on vanadium alloys by exposure to lithium which contained calcium additions [43,44]. Although small micron-sized defects have been observed in many cases, CaO coatings that exhibit good electrical resistance during exposure to lithium at 435°C for >200 h have been produced. Self-healing of these coatings has also been demonstrated by an increase in resistance during lithium exposure after defects in the coating were produced by thermal shock. Further work is required to develop reliable self-healing coatings and to investigate the impact of these coatings on tritium inventory, transport, recovery, and containment.

4. Mechanical properties of irradiated alloys

4.1. Tensile properties

Irradiation of vanadium alloys at temperatures up to 600°C produces significant increases in the yield stress. Although irradiation data at low temperatures are scarce, it appears that the radiation hardening is particularly high at temperatures below 400°C. Fig. 2 summarizes tensile data obtained on V–(4–5%)Cr–(4–5%)Ti alloys as a function of irradiation temperature and damage level [12,45–51]. Similar temperature-dependent hardening behavior has also been observed for irradiated V–2.5Zr–C alloys [51]. Significant radiation hardening is observed at damage levels as low as 0.1 dpa in the low temperature regime (<400°C). The yield strength after irradiation to 0.5 dpa at 100–330°C is higher than that obtained after 10–35 dpa at temperatures above 430°C. The similarity of the yield strengths of V–4Cr–4Ti irradiated at 330°C to 4–6 dpa [12] and 18 dpa [51] implies that the radiation hardening at this relatively low temperature has reached a saturation level already at a dose of ~5 dpa.

A pronounced decrease in the irradiated yield strength occurs for temperatures above ~400°C. Considerable scatter in the strength data is observed near 400°C, which can be attributed to small variations in the nominal vs. actual irradiation temperature, differences in damage level, and heat-to-heat variations in the irradiated alloys. The irradiated yield strength for doses of 10–49 dpa in the high temperature regime (>400°C) decreases slowly with increasing temperature, with appreciable radiation hardening occurring at temperatures up to 600°C. For example, the irradiated yield strength at 600°C is about 60% higher than the unirradiated value (Fig. 2).

All V–(4–5%) Cr–(4–5%) Ti specimens irradiated to doses of 0.1 dpa or higher at irradiation temperatures up to 330°C exhibited pronounced flow localization, with uniform elongations <0.2% in all cases. The uniform elongation slowly increases at temperatures above 400°C, reaching typical values of ~3% at 500°C and ~6% at 600°C for damage levels of 14–35 dpa according to recently revised tensile data [47]. Unfortunately, there are no high-dose (>0.1 dpa) data available in the low-temperature transition regime of 330–400°C. The dramatic decrease in uniform elongation at low irradiation temperatures is due to flow localization. The fracture surfaces of the tensile specimens generally exhibit ductile failure, and the total elongation (~8–10%) and reduction in area (>60%) demonstrate that appreciable plastic deformation occurs in the tensile specimens [12,50].

Two recent TEM studies of the deformation microstructure of V–4Cr–4Ti irradiated at low temperatures

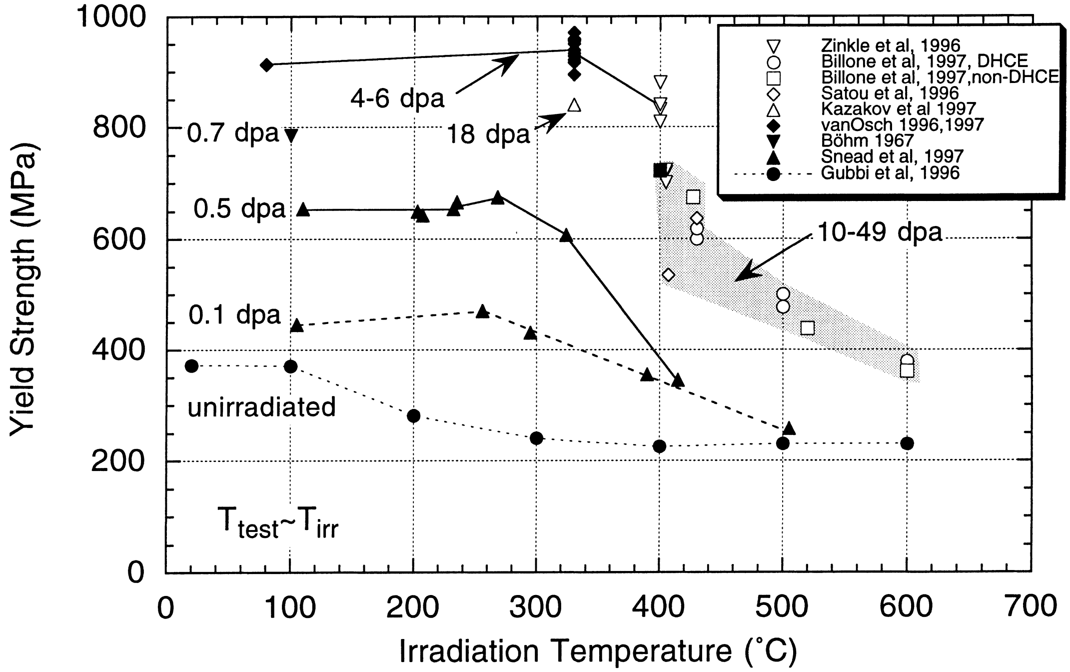

Fig. 2. Temperature-dependent yield strength of unirradiated [9] and irradiated [12,45–51] V–(4–5%) Cr–(4–5%) Ti. The open symbols refer to data obtained in Li-bonded fast reactor irradiation capsules, whereas the filled symbols correspond to unirradiated or mixed spectrum reactor irradiation data.

(200–400°C) have shown that cleared dislocation channels are formed in the interior of the grains [52,53]. Fig. 3 shows an example of dislocation channeling in a deformed specimen that was irradiated at 265°C to 0.5 dpa [53]. Dislocation channeling is a well-known phenomenon in both BCC and FCC metals which have been quenched or irradiated at low temperatures [54–56]. Dislocation channeling occurs because the defect clusters produced during low-temperature irradiation can be easily sheared or otherwise annihilated by dislocations during deformation, i.e., the dislocation barrier strength (α) of the defect clusters is less than the Orowan value of $\alpha = 1$. A recent study found that the barrier strength of the small ($\sim$3 nm diameter) defect clusters produced in V–4Cr–4Ti during low-dose neutron irradiation at temperatures below 300°C was $\alpha \leqslant 0.4$ [57]. A marked transition in the microstructure of V–4Cr–4Ti irradiated to 0.1–0.5 dpa has been observed in the temperature regime near 400°C where the tensile properties show a corresponding large change [53]. Only small dislocation loops were observed at irradiation temperatures below 300°C. However, small Ti-rich precipitates on (0 0 1) habit planes were observed at temperatures above 300°C, and these precipitates were the dominant microstructural feature at elevated temperatures. The large decrease in dislocation loop density and concomitant coarsening of the Ti-rich precipitates at temperatures above 350°C may be responsible for the pronounced decrease in radiation hardening observed in this temperature regime.

Only limited data are available on the strain rate dependence of the tensile properties of irradiated V–(4–5%) Cr–(4–5%) Ti alloys [12,58]. A positive strain rate exponent for the yield strength was observed for

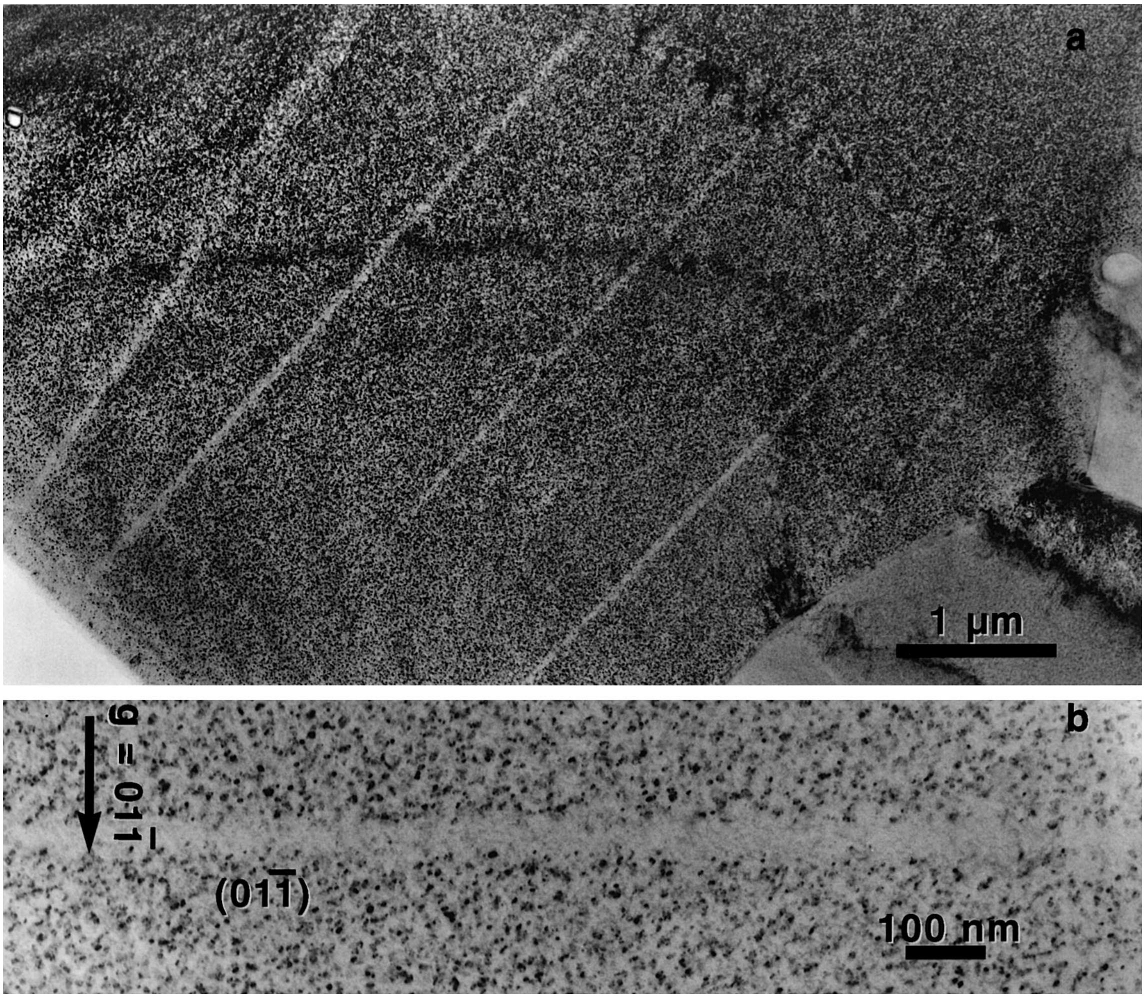

Fig. 3. Cleared dislocation channels in V–4Cr–4Ti irradiated to 0.5 dpa at 275°C and tensile tested at room temperature [53], viewed at low (a) and medium (b) magnification.

specimens irradiated and tested at 200°C, whereas a negative strain rate exponent was observed for specimens irradiated and tested at 400°C [58]. A weak (slightly positive) strain rate exponent was obtained for specimens irradiated and tested at 330°C [12]. These results are in general agreement with the strain rate effects observed on unirradiated specimens [10], suggesting that similar dislocation-interstitial solute interaction mechanisms are operative before and after irradiation.

4.2. Fracture mechanics: Constraint and notch acuity effects

Previous work on unirradiated ferritic/martensitic steels [20] and vanadium alloys [15,21–23,25] has clearly established that Charpy impact or fracture toughness tests performed with machined notches typically produce DBTTs that are significantly lower than the DBTT associated with plane-strain small-scale yielding. This sensitivity to mechanical constraint and notch acuity was established for iron more than 60 years ago [59], and can be even more pronounced following irradiation. Fig. 4 compares the DBTT values obtained from Charpy impact tests on machined-notch (MCVN) and precracked (PCVN) specimens that were irradiated to a dose of 0.5 dpa [50]. The PCVN specimens exhibited DBTT values that were ~50–120°C higher than the corresponding MCVN specimens, with the largest deviations occurring when the measured DBTTs were relatively high. The measured unirradiated DBTTs for the MCVN and PCVN geometries were −200°C and −150°C, respectively [25]. The MCVN specimens used to generate the data in Fig. 4 had a 30° notch with a notch depth of 0.67 mm and a root radius of 0.08 mm. Much of the early published work on the impact properties of unirradiated and irradiated vanadium alloys used a

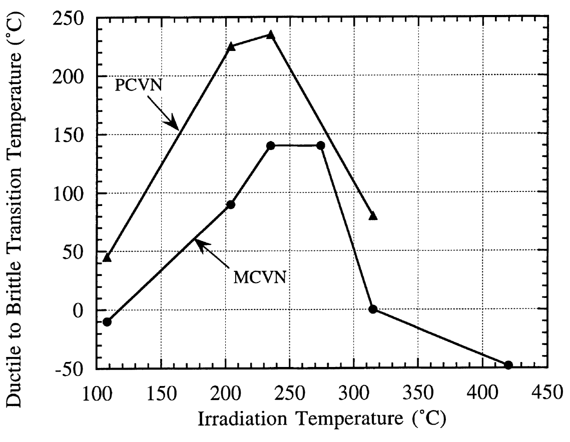

Fig. 4. Comparison of the temperature-dependent DBTT values obtained on V–4Cr–4Ti with machined-notch and precracked CVN specimens irradiated to 0.5 dpa [50].

significantly more blunt-notched specimen with a 45° notch and a root radius of 0.25 mm [5,27]. These blunt-notch DBTT values are lower bounds to what would have been obtained using specimens with sharper notches, and are therefore optimistic (upper-bound) estimates of the DBTT.

An even more serious discrepancy occurs if an estimate of the DBTT is attained from examination of un-notched tensile specimens or TEM disks, as attempted in some recent studies [5,60,61]. To illustrate the potential magnitude of the error associated with this type of approach, it may be noted that all of the tensile specimens irradiated in the same subcapsules as the CVN specimens used to generate the DBTT data in Fig. 4 exhibited ductile fracture surfaces following tensile testing at room temperature [25,50]. Therefore, the estimated DBTT according to the fracture surface morphology of the un-notched tensile specimens would be below room temperature, i.e., more than 120°C lower than the maximum DBTT obtained on MCVN specimens and more than 210°C lower than the maximum DBTT obtained on PCVN specimens. Similarly, a ductile fracture surface was observed on an un-notched V–4Cr–4Ti tensile specimen irradiated to 4 dpa at 400°C and tested at room temperature, even though the DBTT as determined from a MCVN specimen (30° notch, 0.08 mm root radius) was ⩾ 300°C [46]. Fig. 5 shows the fracture surfaces for the tensile and MCVN specimens tested at room temperature and 285°C, respectively. Similar large (>200°C) discrepancies between the DBTT obtained from CVN and un-notched tensile specimens have been obtained on unirradiated V–4Cr–4Ti–0.1Si specimens [17]. These DBTT discrepancies can be mainly attributed to the lack of a notch in the tensile specimens, although differences in strain rate between tensile and Charpy impact tests must also be considered. Clearly, accurate estimates of the DBTT cannot be made without a well-defined notch geometry which serves as the crack initiation site.

Tensile specimens can also provide misleading qualitative information about fracture toughness. Fig. 6 compares the engineering stress–strain curves for two V–4Cr–4Ti specimens which were irradiated to 4 dpa at 400°C and then tensile tested at room temperature and 390°C [46]. The ultimate strength, uniform elongation, and total elongation were all higher in the specimen tested at room temperature, producing a factor of 2.5 higher tensile toughness (defined as the area under the stress–strain curve [62]) compared to the 390°C test. According to MCVN data on the specimen irradiated to 4 dpa at 400°C, the fracture toughness at room temperature should be less than or comparable to that at 390°C, since the DBTT was above 300°C [46] (in conflict with the tensile toughness results, Fig. 6). A similar discrepancy between tensile toughness and fracture toughness at different test temperatures has also been

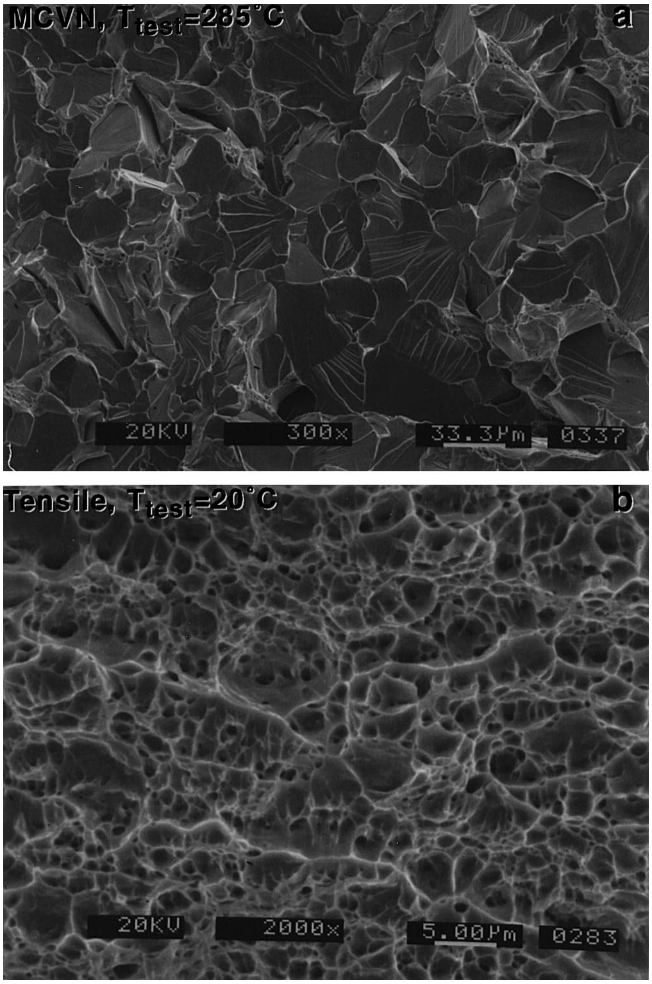

Fig. 5. Fracture surfaces of V–4Cr–4Ti irradiated to 4 dpa at 400°C. (a) Machined-notched CVN specimen tested at 285°C showing transgranular cleavage, and (b) type SS-3 sheet tensile specimen tested at room temperature showing ductile failure [46].

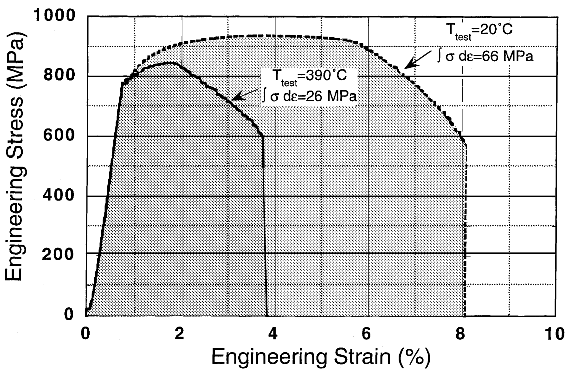

Fig. 6. Engineering stress–strain curves for V–4Cr–4Ti irradiated to 4 dpa at 400°C and tested at room temperature and 390°C [46].

observed in irradiated ferritic/martensitic steels [63]. Therefore, it may be concluded that ductility and toughness measurements obtained on un-notched tensile specimens are misleading indicators of fracture toughness parameters.

According to matrix hardening models for fracture toughness, embrittlement occurs when the local tensile strength exceeds the critical fracture stress. The local tensile stress depends on constraint factors (notch geometry and specimen thickness) which may produce biaxial or triaxial stress states. Cleavage fracture occurs when the critical fracture stress is exceeded over a characteristic minimum distance from the crack tip [22,24]. Fig. 7 shows an example of how the measured yield strength of V–4Cr–4Ti can be correlated with the DBTT measured with machined-notch Charpy specimens [9,23,25,46,50]. This correlation indicates that brittle fracture behavior in unirradiated and irradiated

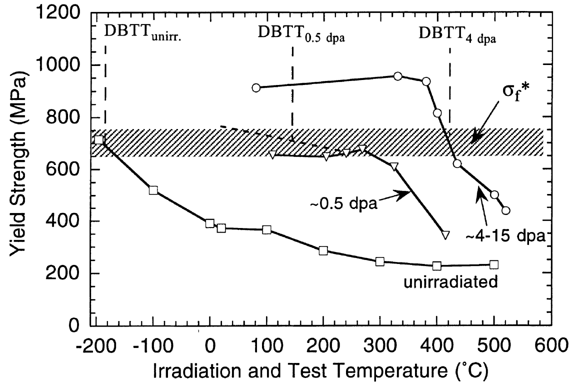

Fig. 7. Correlation between the temperature-dependent yield strength and measured DBTT in unirradiated and irradiated V–4Cr–4Ti specimens.

V–4Cr–4Ti MCVN specimens occurs whenever the yield strength exceeds ~700 MPa. Based on this correlation, the DBTT for V–4Cr–4Ti specimens irradiated to a moderate dose of ~5 dpa would be expected to be very high for irradiation temperatures up to ~400°C, due to the high amount of radiation hardening that occurs at these irradiation temperatures. The sharp decrease in radiation hardening for temperatures above 400°C would reduce the predicted DBTT to values below room temperature, and therefore embrittlement from radiation hardening should be insignificant at operating temperatures above ~430°C. It should be noted that strain rate effects have not been included in this correlation, and that the microscopic critical fracture stress (σ_f) is significantly higher than the microscopic effective yield strength for brittle fracture plotted in Fig. 7 (σ_f*), due to differences in constraint between notched impact specimens and un-notched uniaxial tensile specimens [64]. The main significance of Fig. 7 is that it indicates the DBTT behavior of both unirradiated and irradiated V–4Cr–4Ti is consistent with stress-induced cleavage failure, as predicted by equivalent yield stress models [23,24]. It is also interesting to note that the failure stress in unirradiated and low-temperature irradiated V–4Cr–4Ti specimens was found to be comparable (~1400–1600 MPa) from an analysis of the true stress–true strain tensile curves, in contrast to the large apparent differences which were present in the engineering stress–strain curves [12].

Several microstructural alterations can be considered which could cause an improvement in the tensile elongation of vanadium alloys irradiated at low temperatures. For example, the introduction of a high density of nonshearable (Orowan) obstacles could reduce the amount of dislocation channeling by promoting dislocation multiplication. However, these obstacles would increase the matrix yield strength, which could cause a corresponding increase in the DBTT according to the matrix hardening models for fracture behavior. Cold-worked material would tend to decrease the occurrence of dislocation channeling since many dislocation sources would be available during deformation. A further advantage of cold-working is that it may retard cleavage fracture [65]. Both fracture toughness and tensile specimens must be included in any alloy development program.

5. Critical issues needing further study

In order to build upon the present state of knowledge for vanadium alloys, additional work is needed on several different topics. These can be grouped into studies on unirradiated properties and irradiated properties. In the unirradiated properties category, additional work expanding upon the recent significant advances in joining technology are needed. The ultimate goal of these studies is to develop techniques for joining thick sections of vanadium alloys which do not require post-weld heat treatments (particularly for in-field repairs). An expanded investigation of alternative alloys (low dissolved matrix interstitial solute contents; dispersion or precipitation hardened alloys; oxidation-resistant alloys) would be useful to see if alloys with properties superior to present reference alloys (V–4Cr–4Ti) are possible. Obviously, irradiation studies would need to be performed on any alloys exhibiting promising unirradiated properties. Further work is also needed to develop adherent self-healing insulator coatings which are compatible with vanadium-liquid metal coolant systems.

A key issue regarding radiation effects studies is to determine the minimum and maximum allowable operating temperatures. Further irradiation studies at temperatures between 350°C and 450°C are needed to evaluate the radiation hardening, ductility (reduction in area and tensile elongations), and fracture toughness properties. Damage levels of 1–10 dpa would be suitable for some initial screening studies in this temperature regime. The possible impact of fusion-relevant levels of helium on radiation hardening at higher doses should also be considered. It would also be useful to perform some fundamental studies to determine whether flow localization (dislocation channeling) modifies the relationship between fracture properties and matrix hardening. Additional creep rupture studies on unirradiated [3,66] and irradiated [3] specimens (with and without helium) at test temperatures $\geqslant$ 650°C are needed in order to help establish maximum allowable operating temperatures. Additional work is also needed to determine the magnitude of radiation creep in vanadium alloys, where only limited data are presently available [3,67–69].

6. Conclusions

Significant advances in the production and joining of vanadium alloys have been achieved in the past few years, which further strengthens the technological position of vanadium alloys as an attractive structural material for fusion reactors. Fabrication of large (>500 kg) heats of V–4Cr–4Ti with properties similar to previous small laboratory heats has now been demonstrated. Impressive advances in the joining of thick sections of vanadium alloys using GTA and electron beam welds have been achieved in the past two years, although further improvements are still needed.

The poor work hardening behavior of vanadium alloys at irradiation temperatures below 400°C is due to small defect clusters which can be easily sheared by dislocations during deformation. The concomitant poor fracture properties of vanadium alloys at these low irradiation temperatures is attributable to matrix hardening effects. Microstructural alterations which would improve the tensile elongations of irradiated vanadium alloys (e.g., introduction of nonshearable precipitates) would not necessarily produce any improvement in the fracture properties. The reference lower operating temperature limit for vanadium alloys should be considered to be ~400°C until additional irradiation data become available at temperatures of 350–450°C.

Tensile test ductility and toughness often provide misleading information about the temperature-dependent fracture toughness obtained from Charpy impact or compact tension specimens. A master curve approach analogous to that used in the reactor pressure vessel community has some merits for understanding and applying tensile and fracture toughness data on vanadium alloys as well as other candidate structural materials for fusion reactors. Considerably more specimens are required to develop such master curves than have been traditionally included in irradiation capsule test matrices.

Acknowledgements

This work was sponsored in part by the Office of Fusion Energy Sciences, US Department of Energy, under contract DE-AC05-96OR22464 with Lockheed Martin Energy Research Corp.

References

[1] D.L. Smith, B.A. Loomis, D.R. Diercks, J. Nucl. Mater. 135 (1985) 125.
[2] B.A. Loomis, A.B. Hull, D.L. Smith, J. Nucl. Mater. 179–181 (1991) 148.
[3] B.A. Loomis, D.L. Smith, J. Nucl. Mater. 191–194 (1992) 84.
[4] D.L. Smith, H.M. Chung, B.A. Loomis, H.-C. Tsai, J. Nucl. Mater. 233–237 (1996) 356.
[5] H. Matsui et al., J. Nucl. Mater. 233–237 (1996) 92.
[6] S.N. Votinov et al., J. Nucl. Mater. 233–237 (1996) 370.
[7] W.R. Johnson, J.P. Smith, these Proceedings.
[8] H.M. Chung, L. Nowicki, D.L. Smith, Fusion Materials Semiann. Prog. Report for period ending 30 June 1996, DOE/ER-0313/20, Oak Ridge National Lab, 1996, p. 84.
[9] A.N. Gubbi, A.F. Rowcliffe, W.S. Eatherly, L.T. Gibson, Fusion Materials Semiann. Prog. Report for period ending 30 June 1996, DOE/ER-0313/20, Oak Ridge National Lab, 1996, p. 38.
[10] A.N. Gubbi, A.F. Rowcliffe, to be published.
[11] T. Matsushima, M. Satou, A. Hasegawa, K. Abe, H. Kayano, these Proceedings.
[12] E.V. van Osch, presented at the 8th Int. Conf. on Fusion Reactor Materials, Sendai, 1997.
[13] H. Yoshinaga, K. Toma, K. Abe, S. Morozumi, Philos. Mag. 23 (1971) 1387.
[14] M. Satou, H.M. Chung, Fusion Reactor Materials Semiann. Prog. Report for period ending 30 September 1992, DOE/ER-0313/13, Oak Ridge National Lab, 1992, p. 227.
[15] M.L. Grossbeck, A.F. Rowcliffe, D.J. Alexander, Fusion Materials Semiann. Prog. Report for period ending 31 March 1994, DOE/ER-0313/16, Oak Ridge National Lab, 1994, p. 244.
[16] H. Li, M.L. Hamilton, R.H. Jones, Fusion Materials Semiann. Prog. Report for period ending 31 March 1995, DOE/ER-0313/18, Oak Ridge National Lab, 1995, p. 215.
[17] K. Fukumoto et al., J. Nucl. Mater. 239 (1996) 170.
[18] H.M. Chung, B.A. Loomis, D.L. Smith, J. Nucl. Mater. 239 (1996) 139.
[19] A.F. Rowcliffe, A.N. Gubbi, D.J. Alexander, to be published.
[20] G.E. Lucas, G.R. Odette, J.W. Sheckherd, K. Edsinger, B. Wirth, Fusion Materials Semiann. Prog. Report for Period ending 31 March 1995, DOE/ER-0313/18, Oak Ridge National Lab, 1995, p. 147.
[21] H. Li, R.H. Jones, J.P. Hirth, Fusion Materials Semiann. Prog. Report for period ending 31 March 1994, DOE/ER-0313/16, Oak Ridge National Lab, 1994, p. 279.
[22] G.R. Odette, G.E. Lucas, E. Donahue, J.W. Sheckherd, J. Nucl. Mater. 233–237 (1996) 502.
[23] G.R. Odette, E. Donahue, G.E. Lucas, J.W. Sheckherd, Fusion Materials Semiann. Prog. Report for period ending 30 June 1996, DOE/ER-0313/20, Oak Ridge National Lab, 1996, p. 11.
[24] G.R. Odette et al., presented at the 8th Int. Conf. on Fusion Reactor Materials, Sendai, 1997.
[25] D.J. Alexander et al., in: R.K. Nanstad et al. (Eds.), Eighteenth ASTM Symposium on Effects of Radiation on Materials, ASTM, West Conshohocken, PA, 1998, in press; also Fusion Materials Semiann. Prog. Report for period ending 30 June 1996, DOE/ER-0313/20, Oak Ridge National Lab, 1996, p. 87.
[26] H.M. Chung, L. Nowicki, J. Gazda, D.L. Smith, Fusion Materials Semiann. Prog. Report for Period ending 31 March 1995, DOE/ER-0313/18, Oak Ridge National Lab, 1995, p. 253.

[27] H.M. Chung, L. Nowicki, J. Gazda, D.L. Smith, Fusion Materials Semiann. Prog. Report for period ending 30 September 1994, DOE/ER-0313/17, Oak Ridge National Lab, 1994, p. 183.
[28] H.M. Chung, J. Gazda, L.J. Nowicki, J.E. Sanecki, D.L. Smith, Fusion Materials Semiann. Prog. Report for period ending 30 September 1993, DOE/ER-0313/15, Oak Ridge National Lab, 1993, p. 207.
[29] B.A. Loomis, H.M. Chung, L.J. Nowicki, D.L. Smith, J. Nucl. Mater. 212–215 (1994) 799.
[30] F.A. Garner, L.R. Greenwood, B.A. Loomis, S. Ohnuki, N. Sekimura, J. Nucl. Mater. 233–237 (1996) 406.
[31] A. van Veen, A.V. Federov, A.I. Ryazanov, these Proceedings.
[32] J.F. King, M.L. Grossbeck, G.M. Goodwin, D.J. Alexander, Fusion Materials Semiann. Prog. Report for period ending 31 December 1996, DOE/ER-0313/21, Oak Ridge National Lab, 1996, p. 57.
[33] M.L. Grossbeck, J.F. King, G.M. Goodwin, D.L. Alexander, these Proceedings.
[34] H.M. Chung, R.V. Strain, H.C. Tsai, J.H. Park, D.L. Smith, Fusion Materials Semiann. Prog. Report for period ending 30 June 1996, DOE/ER-0313/20, Oak Ridge National Lab, 1996, p. 55.
[35] J.P. Smith, W.R. Johnson, P.W. Trester, these Proceedings.
[36] J.R. DiStefano, L.D. Chitwood, J.H. DeVan, Fusion Materials Semiann. Prog. Report for period ending 31 December 1995, DOE/ER-0313/19, Oak Ridge National Lab, 1995, p. 54; J.R. DiStefano, J.H. DeVan, J. Nucl. Mater. 249 (1997) 150.
[37] M. Uz, K. Natesan, V.B. Hang, J. Nucl. Mater. 245 (1997) 191.
[38] K. Natesan, W.K. Soppet, M. Uz, these Proceedings.
[39] H.D. Röhrig, J.R. DiStefano, L.D. Chitwood, these Proceedings.
[40] M. Fujiwara, M. Satou, A. Hasegawa, K. Abe, these Proceedings.
[41] D.L. Smith et al., in: Proceedings of IEA Workshop on Liquid Metal Blankets, Paris, 16–18 September 1997, in press.
[42] K. Natesan, C.B. Reed, D.L. Rink, R.C. Haglund, these Proceedings.
[43] J.H. Park, T.F. Kassner, J. Nucl. Mater. 233–237 (1996) 476.
[44] J.H. Park, T.F. Kassner, Fusion Materials Semiann. Prog. Report for period ending 30 June 1996, DOE/ER-0313/20, Oak Ridge National Lab, 1997, p. 111.
[45] H. Böhm, in: International Symposium on Effects of Radiation on Structural Materials, ASTM STP 426, American Society for Testing and Materials, Philadelphia, 1966, p. 95.
[46] S.J. Zinkle et al., Fusion Materials Semiann. Prog. Report for period ending 31 December 1996, DOE/ER-0313/21, Oak Ridge National Lab, 1996, p. 73.
[47] M.C. Billone, H.M. Chung, D.L. Smith, these Proceedings.
[48] M. Satou et al., J. Nucl. Mater. 233-237 (1996) 447.
[49] E.V. van Osch, in: E.V. van Osch (Ed.), Proceedings of Second IEA Workshop on Vanadium Alloy Development for Fusion, ECN-R-96-012, Netherlands Energy Research Foundation ECN, 1996, p. 417.
[50] L.L. Snead, S.J. Zinkle, D.J. Alexander, A.F. Rowcliffe, W.S. Eatherly, Fusion Materials Semiann. Prog. Report for period ending 31 December 1997, DOE/ER-0313/23, p. 81.
[51] V.A. Kazakov, V.P. Chakin, Y.D. Goncharenko, Z.E. Ostrovsky, these Proceedings.
[52] J. Gazda, M. Meshii, H.M. Chung, these Proceedings.
[53] P.M. Rice, S.J. Zinkle, these Proceedings.
[54] M.S. Wechsler, The Inhomogeneity of Plastic Deformation, Am. Society for Metals, Metals Park, OH, 1972, p. 19.
[55] T.J. Koppenaal, R.J. Arsenault, Metall. Rev. 16 (1971) 175.
[56] J.V. Sharp, Radiat. Eff. 14 (1972) 71.
[57] P.M. Rice, L.L. Snead, D.J. Alexander, S.J. Zinkle, in: I.M. Robertson et al. (Eds.), Microstructure Evolution During Irradiation, MRS Symp. Proc., vol. 439, Materials Research Society, Pittsburgh, 1997, p. 343.
[58] S.J. Zinkle, L.L. Snead, J.P. Robertson, Fusion Materials Semiann. Prog. Report for period ending 31 December 1997, DOE/ER-0313/23, 1997, p. 77.
[59] K. Heindlhofer, Trans. AIME 116 (1935) 232.
[60] H.M. Chung, B.A. Loomis, D.L. Smith, J. Nucl. Mater. 233–237 (1996) 466.
[61] H.M. Chung, B.A. Loomis, D.L. Smith, in: D.S. Gelles et al. (Eds.), Seventeenth International Symposium on Effects of Radiation on Materials, ASTM STP 1270, American Society for Testing and Materials, West Conshohocken, PA, 1996, p. 1068.
[62] G.E. Dieter, Mechanical Metallurgy, 2nd ed., McGraw-Hill, New York, 1976, p. 336.
[63] A.F. Rowcliffe et al., these Proceedings.
[64] G.E. Dieter, Mechanical Metallurgy, 2nd ed., McGraw-Hill, New York, 1976, p. 280.
[65] H.M. Chung, H.C. Tsai, D.L. Smith, these Proceedings.
[66] H.M. Chung, B.A. Loomis, D.L. Smith, J. Nucl. Mater. 212–215 (1994) 772.
[67] J.M. Vitek, D.N. Braski, J.A. Horak, J. Nucl. Mater. 141–143 (1986) 982.
[68] V.M. Troyanov et al., J. Nucl. Mater. 233–237 (1996) 381.
[69] H. Tsai, R.V. Strain, H. Matsui, D.L. Smith, these Proceedings.